

## Extended 2,5-Diazaphosphole Oxides: Promising Electron-Acceptor Building Blocks for $\pi$ -Conjugated Organic Materials

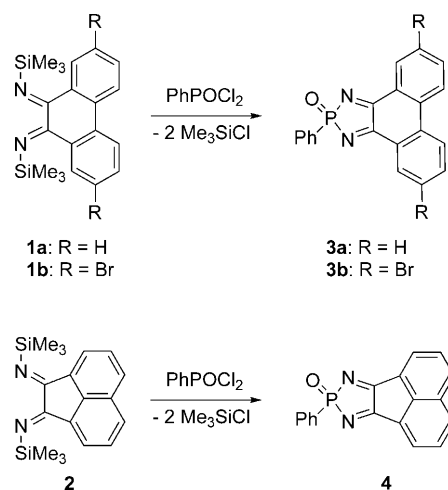
Thomas Linder, Todd C. Sutherland,\* and Thomas Baumgartner\*[a]

The growing need for energy-efficient, low-cost electronics has led to the development of a variety of conceptually new building blocks. A large number of organic  $\pi$ -conjugated materials have now successfully proven their utility for practical applications in organic light-emitting diodes (OLEDs),<sup>[1]</sup> organic field-effect transistors (OFETs),<sup>[2]</sup> and organic photovoltaics (OPVs).<sup>[3]</sup> The significant benefits of using organic components to access semiconducting materials lie in the countless opportunities for fine-tuning the bandgap of the materials through variation of their building-block components.<sup>[4]</sup> One of the most common electron-accepting building-block components in this context is the 2,1,3-benzo[*c*]thiadiazole unit that is utilized in a plethora of molecular and polymeric materials.<sup>[1,3-5]</sup> By using this unit,  $\pi$ -conjugated materials can be formed with low-energy LUMOs that improve the n-type character of materials, or help significantly reduce the bandgap in conjunction with suitable donor building blocks.

In the context of studies on organophosphorus  $\pi$ -conjugated materials, some of us have established the dithieno[3,2-*b*:2',3'-*d*]phosphole system over the past seven years.<sup>[6]</sup> Our studies, and those of others,<sup>[6,7]</sup> have revealed that the incorporation of phosphole units in ring-fused systems afford  $\pi$ -conjugated materials with a variety of beneficial features, one of which is low-lying LUMO energy levels that emphasize their electron-acceptor characteristics. In this communication, we report a new molecular building block that combines the beneficial features of benzothiadiazoles and phospholes to access improved electron-acceptor characteristics. For synthetic reasons, our study focuses on  $\pi$ -extended 2,5-diazaphosphole oxide systems based on acenaph-

thene and phenanthrene backbones and will address general accessibility, as well as their photophysical and electronic properties, including theoretical calculations.

Remarkably, the number of known 2,5-diazaphospholes to date is fairly limited, due to rearrangement reactions of the heterocyclic ring system. Most known systems either exist as W(CO)<sub>5</sub>-complexes, or exhibit donor substituents at the 4,5-position of the ring;<sup>[8]</sup> Dyer and co-workers very recently reported fused diazaphospholes in the context of  $\pi$ -conjugated materials,<sup>[9]</sup> and Rühlmann and co-workers reported the synthesis of two diphenyl-substituted derivatives several decades ago, but no properties were reported.<sup>[10]</sup> Using a similar strategy, we synthesized the  $\pi$ -extended 2,5-diazaphosphole oxides, shown in Scheme 1, from the corresponding



Scheme 1. Synthesis of the 2,5-diazaphosphole oxide derivatives.

phenanthrene and acenaphthene diimines **1a** and **2**. The reactions proceed directly by mixing both reactants without the use of solvent to provide products **3a** and **4** as orange powders in good yields (see the Supporting Information).<sup>[11]</sup> All substances were characterized by NMR spectroscopy, HRMS, and elemental analysis. Interestingly, the <sup>31</sup>P NMR

[a] Dr. T. Linder, Prof. Dr. T. C. Sutherland, Prof. Dr. T. Baumgartner  
Department of Chemistry, University of Calgary  
2500 University Drive NW, Calgary  
AB T2N 1N4 (Canada)  
Fax: (+1) 403-289-9488  
E-mail: todd.sutherland@ucalgary.ca  
thomas.baumgartner@ucalgary.ca

Supporting information for this article is available on the WWW under <http://dx.doi.org/10.1002/chem.201000382>.

shift of the phenanthrene-derived compound **3a** ( $\delta^{31}\text{P} = 76.9$  ppm) differs significantly from that of the acenaphthene derivative **4** ( $\delta^{31}\text{P} = 103.0$  ppm).

Addition of water to the NMR spectroscopy samples neither causes shifting of the  $^{31}\text{P}$  resonances nor the appearance of new signals from decomposition products, which suggests environmental stability. Compounds **3a** and **4** also show good thermal stability; upon heating to  $250^\circ\text{C}$ , neither could mass loss be detected by thermogravimetric analysis (TGA) nor were phase transitions observed with differential scanning calorimetry (DSC). In addition, we have investigated the photophysical properties of the substances by means of fluorescence spectroscopy; both **3a** and **4** are fluorescent in dilute dichloromethane solutions. Compound **4** shows a maximum emission at  $\lambda_{\text{em}} = 495$  nm, which gives a blue-green fluorescence, whereas **3a** reveals an emission maximum of  $\lambda_{\text{em}} = 550$  nm, which results in a yellow fluorescence. The fluorescence spectra of the compounds are shown in the Supporting Information. For both substances, the maximum absorption is found in the UV region at  $\lambda_{\text{max}} = 350$  nm for **3a** and  $\lambda_{\text{max}} = 355$  nm for **4**.

Moreover, single crystals of **3a** suitable for X-ray structure determination were obtained from a concentrated toluene solution.<sup>[12]</sup> As expected, the analysis shows a fused tetracyclic compound, with the phenanthrene backbone and the five membered diazaphosphole unit forming a planar  $\pi$ -conjugated molecular scaffold (Figure 1). The lengths of the

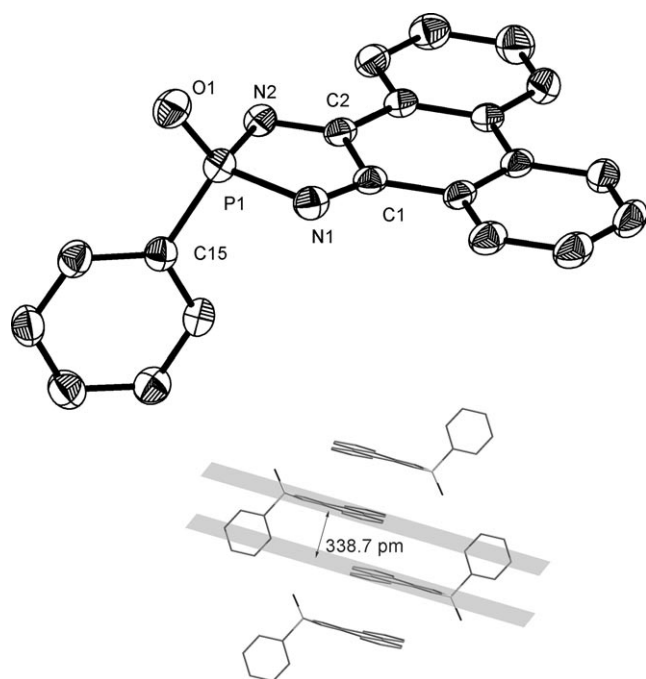


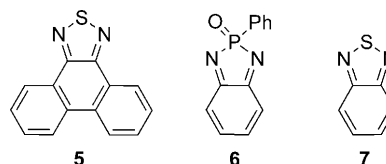
Figure 1. Molecular structure and packing of **3a** in the solid state (50% probability level). The hydrogen atoms are omitted for clarity. Selected bond lengths [pm] and angles [ $^\circ$ ]: P1–N1 171.9(4), P1–N2 170.8(4), P1–O1 147.3(4), P1–C15 179.0(5), N1–C1 128.7(7), N2–C2 128.4(6), C1–C2 151.8(7), N(2)–P(1)–N(1) 98.74(8), C(1)–N(1)–P(1) 105.92(13), C(2)–N(2)–P(1) 106.24(13), N(1)–C(1)–C(2) 114.55(16), N(2)–C(2)–C(1) 114.53(16).

C–N bonds (128.7(7) and 128.4(6) pm) are clearly in the range of double bonds, whereas the P–N bonds (171.9(4) and 170.8(4) pm) and the C–C bond (151.8(7) pm) in the five-membered ring possess bond lengths typical for single bonds involving pentavalent P-species.<sup>[8a,c]</sup>

The molecular packing of **3a** in the solid state supports stacks of molecules that are stabilized by  $\pi$ – $\pi$  interactions (Figure 1). The nonplanar parts of the molecule arrange in an alternating manner. The stacking distance between two molecules is found to be 338.7 pm, which is significantly shorter than the parent 9,10-phenanthrenequinone (351.5 pm),<sup>[13]</sup> or phenanthro[9,10-*c*]-1,2,5-thiadiazole oxide (349.5 pm).<sup>[14]</sup>

We also succeeded in accessing the brominated species **3b** ( $\delta^{31}\text{P} = 76.7$  ppm) through a similar protocol by using the dibrominated diimine **1b** (Scheme 1), however, the fluorescence of **3b** was found to be negligible, which is likely to be due to the heavy atom effect of bromine. The synthesis of **3b** nevertheless proves that access to a functional component is possible and that it could be employed in organic materials through, for example, cross-coupling procedures. Efforts to reduce the pentavalent phosphorus center in **3a** and **4** for further manipulation of the electronic properties of the scaffold, however, were found to be challenging. Even with a range of reductants ( $\text{BH}_3/\text{NMe}_3$ ,  $\text{HSiCl}_3$ ,  $\text{PBU}_3$ ) that have successfully been used for this purpose in related systems,<sup>[6c,7]</sup> clean and selective P-reduction could not be achieved.

To better understand the observed features for the extended 2,5-diazaphospholes **3a** and **4**, we have performed DFT calculations (B3LYP/6-31G(d+) level of theory)<sup>[15]</sup> on the neutral species, as well as their radical anions. For comparison, we have also included the corresponding sulfur analogue **5**,<sup>[10a]</sup> as well as the parent phosphorus and sulfur benzo-systems **6** and **7** (Scheme 2).



Scheme 2. Additional compounds used for comparison in the DFT calculations.

The calculations on the parent systems reveal that the replacement of the sulfur in benzothiadiazole (**7**) by a phosphoryl group (**6**) has a significant effect on the energy level of the LUMO. The LUMO of **6** is more than 1 eV lower than the LUMO of the sulfur analogue **7** (**6**:  $E = -3.87$  eV, **7**:  $E = -2.67$  eV), but the HOMO energy levels of **6** and **7** are similar (**6**:  $E = -7.04$  eV, **7**:  $E = -6.89$  eV). The same is true for the extended systems (see the Supporting Information). The low-lying LUMO energy levels in **3a** ( $E = -3.03$  eV; cf., **5**:  $E = -2.01$  eV, **4** ( $E = -2.60$  eV), and **6** correlate with those of native phosphole derivatives and can be

attributed to an interaction of the  $\sigma^*$  orbital of the exocyclic substituents at phosphorus with the  $\pi^*$  orbital of the conjugated main scaffold.<sup>[7]</sup> Despite the different energy levels, the shape of the LUMOs (and other relevant frontier orbitals) is almost identical in both the phosphorus and sulfur species, which supports the strong correlation between these systems. Importantly, upon reduction to the radical anions, the frontier orbitals retain their shape in both families; this indicates that the radical is easily delocalized within the  $\pi$  system without affecting the molecular integrity of the scaffold. It is interesting to note, however, that the spin densities of the phosphorus-based systems are significantly different to both of the sulfur species **5** and **7**. In **3a** and **4**, a large portion of the spin density is located at the carbon atoms of the diazaphosphole subunit, but only little spin density is found on the phosphorus center, which supports the presence of a diazabutadiene radical anion fragment (see the Supporting Information). In stark contrast, the spin density of the sulfur analogue **5** is mostly located on the  $\text{SN}_2$  fragment. This difference in spin density distribution can also explain the observed variances in the electrochemical reduction of **3a**, **4**, and **7** (see below), which supports a much more delocalized and stable radical anion for the P-systems.

To verify the electron-acceptor characteristics of the diazaphosphole oxides, we have performed cyclic voltammetry using **3a** and **4** and compared the results with the performance of 2,1,3-benzo[*c*]thiadiazole **7**. Compound **3a** shows quasireversible redox behavior at various scan rates, which indicates the occurrence of stable redox switching (Figure 2a). The average of the anodic and cathodic peak poten-

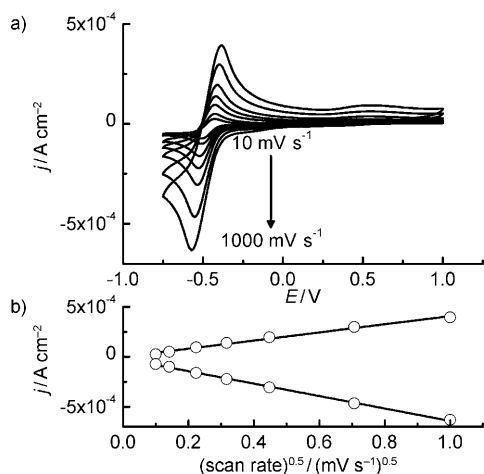


Figure 2. Cyclic voltammogram of **3a** (3.1 mM) in DMF containing  $\text{Bu}_4\text{NPF}_6$  (0.1 M) obtained by using a glass carbon working electrode, a  $\text{Ag} | \text{AgCl} | \text{KCl}_{3\text{M}}$  reference electrode, and a Pt wire counter electrode.

tials provides an estimate of the  $E_{1/2}$  value of  $-949$  mV (vs.  $\text{Fc}/\text{Fc}^+$ ). For comparison, under the same conditions **4** and **7** have significantly lower  $E_{1/2}$  values of  $-1224$  and  $-1257$  mV, respectively. Matano and co-workers<sup>[16]</sup> recently reported an acenaphtho[1,2-*c*]phosphole P-oxide with a reduction potential of  $-1820$  mV (vs.  $\text{Fc}/\text{Fc}^+$ ) that displayed the highest re-

ported electron mobility of  $8 \times 10^{-5} \text{ cm}^2 \text{ V}^{-1} \text{ s}^{-1}$  (at  $E = 10^6 \text{ V cm}^{-1}$ ) for phosphole P-oxides, which demonstrates the prospects for **3** and **4** in similar applications.

Figure 2b demonstrates that compound **3a** operates under diffusion control and is not absorbing to the electrode surface and the linear fit is used to extract the diffusion coefficient of  $4.4 \times 10^{-7} \text{ cm}^2 \text{ s}^{-1}$ , according to the Randles–Sevcik equation.<sup>[17]</sup> Note that compounds **4** and **7** also show a linear relationship between the square root of scan rate and peak current. By using Nicholson's method,<sup>[18]</sup> the anodic ( $E_{\text{pa}}$ ) and cathodic ( $E_{\text{pc}}$ ) peak separation is correlated with the apparent electron-transfer rate constant,  $k_{\text{app}}$ , resulting in a moderate rate of  $9.6 \times 10^{-4} \text{ cm s}^{-1}$  for **3a**. To compare, compounds **4** and **7** have  $k_{\text{app}}$  values of  $4.4 \times 10^{-4} \text{ cm s}^{-1}$  and  $3.1 \times 10^{-4} \text{ cm s}^{-1}$ , respectively. The electrochemical results show that both **3a** and **4** are easier to reduce than benzothiadiazole **7** and possess competitive electron-transfer characteristics, which could lead to improved n-type materials.

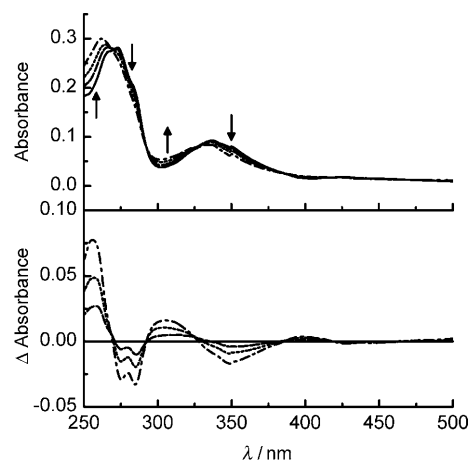


Figure 3. UV/Vis spectroelectrochemistry of **3a** at various time periods of  $-0.7$  V applied potential. Top: UV/Vis absorption profile of **3a** at 0 (—), 5 (---), 10 (----), and 15 (---) minute intervals after an applied  $-0.7$  V potential. The arrows indicate the direction of peak movement. Bottom: The absorption difference spectra, initial spectra were subtracted from each of the spectra at the indicated time intervals, which clearly show the radical anion spectral evolution and isosbestic points.

Figure 3 is the UV/Vis spectroelectrochemical result of reducing **3a** to the radical anion  $\mathbf{3a}^{\cdot -}$ . The initial UV/Vis absorption spectrum of **3a** consists of two main features: a strong  $\pi$ - $\pi^*$  transition at 275 nm and a weaker  $n$ - $\pi^*$  transition at 330 nm. A negative potential of  $-0.7$  V was applied to the spectroelectrochemical cell and UV/Vis spectra were recorded every 5 min. The absorption difference spectra, shown at the bottom of Figure 3, illustrate clear isosbestic points that support a clean conversion to the radical anion. In addition, the negative growing peaks of Figure 3 can be clearly correlated with neutral **3a**, whereas the new spectral features appearing at 260 nm and 310 nm can be assigned to the  $\pi$ - $\pi^*$  and  $n$ - $\pi^*$  transitions of the radical anion. The blueshift in the radical anion structure is consistent with the DFT-calculated HOMO–LUMO energy gaps of  $\mathbf{3a}^{\cdot -}$ .

Furthermore, compound **3a** was reduced chemically with Na in THF at room temperature, yielding a purple solution of the stable radical anion **3a<sup>-•</sup>** that was subjected to EPR spectroscopy (Figure 4). The observed  $g_{\text{iso}}$  value of 2.0049 is

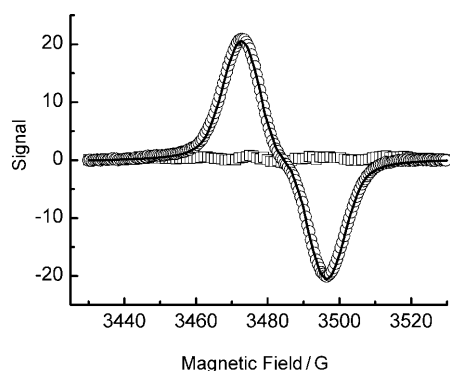


Figure 4. EPR spectra of **3a<sup>-•</sup>** in THF at room temperature (open circles: experimental; line: simulated; open squares: residuals).

typical of thiadiazole- and phosphole-based ring systems.<sup>[19]</sup> To verify the observed results, the EPR spectrum was also modeled by using Winsim2002 providing a goodness of fit of 99.9% with the experimental data.<sup>[20]</sup> The DFT-calculated hyperfine coupling constants for the radical anion **3a<sup>-•</sup>** were used as starting values for the simulation (for details, see the Supporting Information).

In conclusion, we have demonstrated the convenient synthesis of  $\pi$ -extended 2,5-diazaphosphole oxides that can be considered as phosphorus analogues of the very popular 2,1,3-benzo[c]thiadiazole-based materials. Theoretical calculations, as well as electrochemical studies have revealed that the phosphorus-based systems show favorable reduction features (reduction potential and electron-transfer rates) over those of the ubiquitous benzothiadiazole, even in their  $\pi$ -extended forms. The DFT calculations further support the strong correlation between the two classes of compounds, but also indicated a different spin density distribution in the radical anion that is very likely to be the reason for the greater stability of the P-based radical anions. Our studies have revealed that the replacement of the sulfur by a phosphoryl group affords materials that have dramatically improved electron-acceptor characteristics that are highly desirable for the next generation of organic electronic materials. We are currently exploring the scope of potential applications by incorporating the novel extended 2,5-diazaphospholes into an array of different  $\pi$ -conjugated materials.

### Acknowledgements

Financial support by NSERC of Canada, the Canada Foundation of Innovation, and the Institute of Sustainable Energy, Environment and Economy (ISEEE) is gratefully acknowledged. T.B. thanks Alberta Ingenuity for a New Faculty Award. We also thank T. K. Wood for helpful discussions regarding the EPR spectroscopy.

**Keywords:** conjugation • density functional calculations • electron acceptor • organic electronics • phosphorus heterocycles

- [1] a) *Organic Light Emitting Devices* (Eds.: K. Müllen, U. Scherf), Wiley-VCH, Weinheim, **2005**; b) *Handbook of Conducting Polymers*, 3rd ed. (Eds.: T. A. Skotheim, J. R. Reynolds), CRC Press, Boca Raton, **2006**.
- [2] a) C. D. Dimitrakopoulos, P. R. L. Malenfant, *Adv. Mater.* **2002**, *14*, 99; b) J. E. Anthony, *Angew. Chem.* **2008**, *120*, 460; *Angew. Chem. Int. Ed.* **2008**, *47*, 452; c) A. R. Murphy, J. M. J. Fréchet, *Chem. Rev.* **2007**, *107*, 1066; d) S. Allard, M. Forster, B. Souharce, H. Thiem, U. Scherf, *Angew. Chem.* **2008**, *120*, 4138; *Angew. Chem. Int. Ed.* **2008**, *47*, 4070.
- [3] a) B. C. Thompson, J. M. J. Fréchet, *Angew. Chem.* **2008**, *120*, 62; *Angew. Chem. Int. Ed.* **2008**, *47*, 58; b) S. Günes, H. Neugebauer, N. S. Sariciftci, *Chem. Rev.* **2007**, *107*, 1324.
- [4] See, for example: a) J. Roncali, *Chem. Rev.* **1997**, *97*, 173; b) J. Roncali, *Macromol. Rapid Commun.* **2007**, *28*, 1761; c) A. C. Grimsdale, K. L. Chan, R. E. Martin, P. G. Jokisz, A. B. Holmes, *Chem. Rev.* **2009**, *109*, 897; d) A. Mishra, C.-Q. Ma, P. Bäuerle, *Chem. Rev.* **2009**, *109*, 1141.
- [5] For some recent examples, see: a) C. V. Hoven, A. Garcia, G. C. Bazan, T.-Q. Nguyen, *Adv. Mater.* **2009**, *21*, 3793; b) K. M. Omer, S.-Y. Ku, K.-T. Wong, A. J. Bard, *J. Am. Chem. Soc.* **2008**, *130*, 10733; c) L. Biniek, C. L. Chochos, N. Leclerc, G. Hadziioannou, J. K. Kallitsis, R. Bechara, P. Lévêque, T. Heiser, *J. Mater. Chem.* **2009**, *19*, 4946; d) M.-H. Chen, J. Hou, Z. Hong, G. Yang, S. Sista, L.-M. Chen, Y. Yang, *Adv. Mater.* **2009**, *21*, 4238; e) A. L. Appleton, S. Miao, S. M. Brombosz, N. J. Berger, S. Barlow, S. R. Marder, B. M. Lawrence, K. I. Hardcastle, U. H. F. Bunz, *Org. Lett.* **2009**, *11*, 5222.
- [6] a) T. Baumgartner, T. Neumann, B. Wirges, *Angew. Chem.* **2004**, *116*, 6323; *Angew. Chem. Int. Ed.* **2004**, *43*, 6197; b) T. Baumgartner, W. Bergmans, T. Kárpáti, T. Neumann, M. Nieger, L. Nyulászi, *Chem. Eur. J.* **2005**, *11*, 4687; c) Y. Dienes, S. Durben, T. Kárpáti, T. Neumann, U. Englert, L. Nyulászi, T. Baumgartner, *Chem. Eur. J.* **2007**, *13*, 7487; d) Y. Dienes, M. Eggenstein, T. Kárpáti, T. C. Sutherland, L. Nyulászi, T. Baumgartner, *Chem. Eur. J.* **2008**, *14*, 9878; e) Y. Ren, Y. Dienes, S. Hettel, M. Parvez, B. Hoge, T. Baumgartner, *Organometallics* **2009**, *28*, 734; f) C. Romero-Nieto, S. Merino, J. Rodríguez-López, T. Baumgartner, *Chem. Eur. J.* **2009**, *15*, 4135.
- [7] a) Y. Matano, H. Imahori, *Org. Biomol. Chem.* **2009**, *7*, 1258; b) A. Fukazawa, S. Yamaguchi, *Chem. Asian J.* **2009**, *4*, 1386; c) J. Crasous, R. Réau, *Dalton Trans.* **2008**, 6865; d) T. Baumgartner, R. Réau, *Chem. Rev.* **2006**, *106*, 4681 (correction: T. Baumgartner, R. Réau, *Chem. Rev.* **2007**, *107*, 303); e) F. Mathey, *Angew. Chem.* **2003**, *115*, 1616; *Angew. Chem. Int. Ed.* **2003**, *42*, 1578.
- [8] a) H. Wilkens, J. Jeske, P. G. Jones, R. Streubel, *Chem. Commun.* **1997**, 2317; b) H. Wilkens, F. Ruthe, P. G. Jones, R. Streubel, *Chem. Eur. J.* **1998**, *4*, 1542; c) A. A. Khan, C. Neumann, C. Wismach, P. G. Jones, R. Streubel, *J. Organomet. Chem.* **2003**, 682, 212.
- [9] a) D. A. Smith, A. S. Batsanov, K. Miqueu, J.-M. Sotiropoulos, D. C. Apperley, J. A. K. Howard, P. W. Dyer, *Angew. Chem.* **2008**, *120*, 8802; *Angew. Chem. Int. Ed.* **2008**, *47*, 8674; b) D. A. Smith, A. S. Batsanov, M. A. Fox, A. Beeby, D. C. Apperley, J. A. K. Howard, P. W. Dyer, *Angew. Chem.* **2009**, *121*, 9273; *Angew. Chem. Int. Ed.* **2009**, *48*, 9109.
- [10] a) G. Truchtenhagen, K. Rühlmann, *Liebigs Ann. Chem.* **1968**, 711, 174; b) H. Buchwald, K. Rühlmann, *J. Organomet. Chem.* **1979**, 166, 25.
- [11] Only with the pentavalent phosphorus species does the reaction lead to the desired diazaphosphole framework. The use of trivalent phosphorus synthons affords an inseparable mixture of compounds, none of which could be identified as diazaphosphole species.
- [12] Crystal data for **3a**: (C<sub>20</sub>H<sub>13</sub>N<sub>2</sub>OP):  $M_r = 328.29$ ;  $T = 173(2)$  K; monoclinic, space group  $P2_1/c$ ;  $a = 7.3950(10)$ ,  $b = 9.6610(10)$ ,  $c = 22.339(2)$  Å;  $\beta = 96.695(2)^\circ$ ;  $V = 1585.1(3)$  Å<sup>3</sup>;  $Z = 4$ ;  $\rho_{\text{calcd}} =$

1.376 mg m<sup>-3</sup>;  $\mu=0.182$  mm<sup>-1</sup>;  $\lambda=0.71070$  Å;  $\theta_{\max}=27.41^\circ$ ; 5244 measured reflections; 3258 [ $R(\text{int})=0.0179$ ] independent reflections; GOF on  $F^2=1.195$ ;  $R_1=0.0439$ ;  $wR_2=0.1237$  ( $I>2\sigma(I)$ );  $R_1=0.0494$ ;  $wR_2=0.1286$  (for all data); largest difference peak and hole 0.277 and  $-0.345$  e Å<sup>-3</sup>. The intensity data were collected on a Nonius KappaCCD diffractometer with graphite monochromated MoK $\alpha$  radiation. The structure was solved by direct methods (SHELXTL) and refined on  $F^2$  by full-matrix least-squares techniques. Hydrogen atoms were included by using a riding model. CCDC-753279 contains the supplementary crystallographic data for this paper. These data can be obtained free of charge from The Cambridge Crystallographic Data Centre via [www.ccdc.cam.ac.uk/data\\_request/cif](http://www.ccdc.cam.ac.uk/data_request/cif).

- [13] S. K. Arora, *Acta Crystallogr. Sect. B* **1974**, *30*, 2923.
- [14] S. Y. Matsuzaki, M. Gotoh, A. Kuboyama, *Mol. Cryst. Liq. Cryst.* **1987**, *142*, 127.
- [15] Gaussian 03, Revision E.01, M. J. Frisch, G. W. Trucks, H. B. Schlegel, G. E. Scuseria, M. A. Robb, J. R. Cheeseman, J. A. Montgomery, Jr., T. Vreven, K. N. Kudin, J. C. Burant, J. M. Millam, S. S. Iyengar, J. Tomasi, V. Barone, B. Mennucci, M. Cossi, G. Scalmani, N. Rega, G. A. Petersson, H. Nakatsuji, M. Hada, M. Ehara, K. Toyota, R. Fukuda, J. Hasegawa, M. Ishida, T. Nakajima, Y. Honda, O. Kitao, H. Nakai, M. Klene, X. Li, J. E. Knox, H. P. Hratchian, J. B. Cross, V. Bakken, C. Adamo, J. Jaramillo, R. Gomperts, R. E. Stratmann, O. Yazyev, A. J. Austin, R. Cammi, C. Pomelli, J. W. Ochterski, P. Y. Ayala, K. Morokuma, G. A. Voth, P. Salvador, J. J. Dannenberg, V. G. Zakrzewski, S. Dapprich, A. D. Daniels, M. C. Strain, O. Farkas, D. K. Malick, A. D. Rabuck, K. Raghavachari, J. B. Foresman, J. V. Ortiz, Q. Cui, A. G. Baboul, S. Clifford, J. Cio-slawski, B. B. Stefanov, G. Liu, A. Liashenko, P. Piskorz, I. Komaromi, R. L. Martin, D. J. Fox, T. Keith, M. A. Al-Laham, C. Y. Peng, A. Nanayakkara, M. Challacombe, P. M. W. Gill, B. Johnson, W. Chen, M. W. Wong, C. Gonzalez, J. A. Pople, Gaussian Inc., Wallingford, CT, **2007**.
- [16] A. Saito, T. Miyajima, M. Nakashima, T. Fukushima, H. Kaji, Y. Matano, H. Imahori, *Chem. Eur. J.* **2009**, *15*, 10000.
- [17] A. J. Bard, L. R. Faulkner, *Electrochemical Methods: Fundamentals and Applications*, 2nd ed., Wiley, New York, **2001**.
- [18] R. S. Nicholson, *Anal. Chem.* **1965**, *37*, 1351.
- [19] a) C. L. Kwan, M. Carmack, J. K. Kochi, *J. Phys. Chem.* **1976**, *80*, 1786; b) P. Adkine, T. Cantat, E. Deschamps, L. Ricard, N. Mezzailles, P. Le Floch, M. Geoffroy, *Phys. Chem. Chem. Phys.* **2006**, *8*, 862; c) R. Edge, R. J. Less, E. J. L. McInnes, K. Mütther, V. Naseri, J. M. Rawson, D. S. Wright, *Chem. Commun.* **2009**, 1691.
- [20] P. E. S. T. Winsim, V.1.0, National Institute of Environmental Health Sciences National Institutes of Health (USA), **2002**, <http://epr.niehs.nih.gov/>; D. R. Duling, *J. Magn. Reson. Ser. B* **1994**, *104*, 105.

Received: February 11, 2010  
Published online: May 12, 2010